sustainability

MDPI

Article

First and Second Law Analyses of Trans-critical N_2O Refrigeration Cycle Using an Ejector

Damoon Aghazadeh Dokandari [1], S. M. S. Mahmoudi [2,*], M. Bidi [1], Ramin Haghighi Khoshkhoo [1] and Marc A. Rosen [3]

1 Faculty of Mechanical and Energy Engineering, Shahid Beheshti University, A.C., Tehran 16765-1719, Iran; D_Aghazadeh@sbu.ac.ir (D.A.D.); M_bidi@sbu.ac.ir (M.B.); R_haghighi@sbu.ac.ir (R.H.K.)
2 Faculty of Mechanical Engineering, Tabriz University, Tabriz 51666-14766, Iran
3 Faculty of Engineering and Applied Science, University of Ontario Institute of Technology, 2000 Simcoe Street North, Oshawa, Ontario L1H 7K4, Canada; Marc.Rosen@uoit.ca
* Correspondence: s_mahmoudi@tabrizu.ac.ir

Received: 18 February 2018; Accepted: 9 April 2018; Published: 13 April 2018

Abstract: An ejector-expansion refrigeration cycle using nitrous oxide was assessed. Thermodynamic analyses, including energy and exergy analyses, were carried out to investigate the effects on performance of several key factors in the system. The results show that the ejector-expansion refrigeration cycle (EERC) has a higher maximum coefficient of performance and exergy efficiency than the internal heat exchanger cycle (IHEC), by 12% and 15%, respectively. The maximum coefficient of performance and exergy efficiency are 14% and 16.5% higher than the corresponding values for the vapor-compression refrigeration cycle (VCRC), respectively. The total exergy destruction for the N_2O ejector-expansion cycle is 63% and 53% less than for IHEC and VCRC, respectively. Furthermore, the highest COPs for the vapor-compression refrigeration, the internal heat exchanger and the ejector-expansion refrigeration cycles correspond to a high side pressure of 7.3 MPa, and the highest COPs for the three types of CO_2 refrigeration cycles correspond to a high side pressure of 8.5 MPa. Consequently, these lead to a lower electrical power consumption by the compressor.

Keywords: refrigeration cycle; ejector; nitrous oxide; COP; exergy

1. Introduction

Various refrigerants are used presently in vapor compression refrigeration cycles. However, concerns have been repeatedly raised about many refrigerants, due to their environmental characteristics such as ozone depletion potential, global warming potential and atmospheric lifetime (ALT). Natural refrigerants have recently been recognized to have promise over artificial ones because of several beneficial characteristics. For example, CO_2, one type of natural refrigerant, is non-flammable, non-toxic and non-corrosive fluid. Nitrous oxide (N_2O) is a non-toxic fluid, albeit with a somewhat higher global warming potential than CO_2 [1,2]. It has thermodynamic similarities in critical temperature and pressure and molar weight with carbon dioxide, and could be replaced with CO_2. N_2O has a critical temperature, boiling point and triple point of 36.4, −88.5 and −90.82 °C, respectively [3]. The use of ejectors in refrigeration systems has been practiced by many investigators, in large part because they do not have moving parts and need no work for compression. These components reduce exergy destruction and can be utilized when there are three pressure levels in a system.

Numerous investigations have been reported of vapor compression refrigeration cycles using natural refrigerants. Deng et al. [4] performed a theoretical analysis of a trans-critical CO_2 refrigeration cycle with an ejector, and studied the relation between ejector entrainment ratio and vapor quality at the

outlet of the ejector. The results showed that the entrainment ratio decreases as compressor discharge pressure increases, which is the opposite of what was observed for vapor quality. Moreover, the authors concluded that the system has an optimum entrainment ratio corresponding to the maximum COP for the system.

Sadeghi et al. [5] proposed a novel multi-generation hybrid system and analyzed it in detail thermodynamically. Using a zeotropic mixture as a working fluid, the system consists of power and ejector refrigeration cycles as well as a desalination system based on humidification and dehumidification processes. The results in the first case reveal a maximum overall exergy efficiency of 17.12% for which the net output power is 57.03 kW and the refrigeration capacity is 91.25 kW. In the case of multi-objective optimization, the results obtained from the Pareto frontier show a net produced power of 52.19 kW and a refrigeration capacity of 120.4 kW. Unal et al. [6] developed a model to predict the optimal thermodynamic parameters for a two-phase ejector refrigeration system for buses using R134a under various operating conditions. The study revealed that the heat transfer surface areas can be reduced by about 4% and 55% in the condenser and evaporator, respectively.

Sarkar and Bhattacharyya [7] thermodynamically optimized the compressor discharge pressure in a conservative trans-critical N_2O refrigeration cycle, and investigated the effect of superheating in the evaporator, internal heat exchange and the use of a recovery turbine instead of an expansion valve on cycle behavior. They also compared the cycle with a CO_2 refrigerant cycle, and found that the trans-critical N_2O cycle has a higher cooling coefficient of performance, a lower compressor pressure ratio, and a lower discharge pressure and temperature than the carbon dioxide refrigerant cycle. Aghazadeh Dokandari et al. [8] investigated a novel configuration for ejector expansion in a CO_2/NH_3 cascade cycle, and performed first and second law analyses of its performance; the theoretical analysis of the functional features based on the first and second laws of the thermodynamics illustrated that the maximum COP and the maximum second law efficiency are on average 7% and 5%, respectively, higher than for the conventional cycle.

Croquer et al. [9] systematically compared ejector performances using thermodynamic and CFD approaches for various operating conditions. The thermodynamic model predicted higher entrainment ratios for double choking operation and somewhat different values of the critical and limiting pressure ratios.

Sarkar and Bhattacharyya [10–12] studied several uses of trans-critical N_2O and CO_2 as refrigerants in various configurations for heating and refrigeration and optimized the cycles.

Candeniz Seckin [13] investigated a novel power and refrigeration cycle, which combines a Kalina cycle and an ejector refrigeration cycle (ERC). The results showed that thermal efficiency of the combined cycle increases with increasing turbine inlet temperature and concentration of ammonia–water solution, but decreases with rising condenser outlet temperature and heat exchanger pressure. Lee et al. [14] examined the optimum condensation temperature for the cascade-condenser in CO_2/NH_3 cascade refrigeration systems to obtain the lowest exergy destruction and the highest COP.

Carrillo et al. [15] showed the potential benefits of using ejectors in cooling systems to improve energy efficiency. They compared different configurations of ejector cooling systems with a conventional compressor cycle. Considering a range of condenser temperature T_{con} (43–53°C) and of an evaporator temperature T_{eva} (3–11°C), they showed that the coefficient of performance could increase by up to 26%.

Rashidi et al. [16] described the performance of an ejector refrigeration cycle using R600 as a working fluid. The evaporator, generator and condenser are assumed as heat exchangers that exchange heat with three external fluids. Furthermore, Yari and Mahmoudi [17] proposed and analyzed two cascade refrigeration cycles, with an ejector-expansion cycle and a subcritical CO_2 cycle in the top and bottom portions of both cycles, respectively. Yari [18] also studied the performance of a novel two-stage ejector-expansion trans-critical refrigeration cycle.

Ghaebi et al. [19] proposed a novel combined power and ejector refrigeration cycle using an appropriate combination of a Kalina cycle (KC) and an ejector refrigeration cycle (ERC) to produce

power and cooling, simultaneously. The optimum thermal efficiency, exergy efficiency, and SUCP of the system are calculated to be 20.4%, 16.7%, and 2466 $/MWh, respectively.

Jeon et al. [20] proposed a novel combined power and ejector refrigeration cycle comprised of an appropriate combination of a KC and an ejector refrigeration cycle to produce power and cooling, simultaneously. Yinhai et al. [21] studied a theoretical model of an ejector for a trans-critical carbon dioxide ejector-expansion refrigeration system capable of predicting the mass flow rates of both primary and secondary flows. A non-equilibrium correlation in the energy-conservation equation was proposed and validated using 130 cases obtained from three ejector configurations.

Fang et al. [22] reported a numerical analysis of a single-phase supersonic ejector working with R134a as well as hydrofluoroolefin (HFO) refrigerants R1234yf and R1234ze(E). Note that using R1234ze(E) would induce some modifications due to its thermodynamic properties. Maintaining the same pressure ratio for the ejector would lead on the one hand to a better entrainment ratio using R1234ze(E) and on the other hand to a reduced coefficient of performance (COP) and cooling power, by 4.2% and 26.6% on average, respectively. Using R1234yf under the same conditions induced an average decrease of 5.2% for the entrainment ratio, 9.6% for the COP and 19.8% for the cooling power. Ma et al. [23] presented a detailed thermodynamic modelling method for an ejector in an ejection refrigeration system. In this model, the primary flow in the ejector is assumed to fan out from the nozzle without mixing with the secondary flow in a certain downstream distance, so that a hypothetical throat is formed where the secondary flow reaches the speed of sound.

Choudhary et al. [24] analyzed a novel N_2O based trans-critical refrigeration system in which an ejector is used as an expansion device. Their system is found to have a higher COP, a lower compressor discharge pressure and a higher entrainment ratio but suffers from having a lower volumetric cooling capacity. They reported that the maximum COP is about 10% higher compared to the case when CO_2 is used as a working fluid.

The above review clearly shows the significance of ejectors in energy conversion systems and, in particular, for refrigeration devices. In addition, the use of N_2O has attracted the attention of investigators because of some advantageous features in its thermodynamic properties. To the authors' knowledge, the use of N_2O in a trans-critical refrigeration cycle with an ejector has not been investigated thermodynamically yet and the present work addresses this lack of information. This investigation aims to improve understanding of the system, and help in comparing its performance with the performances of other refrigeration system.

2. System Description

Three configurations for the trans-critical N_2O refrigeration cycle are considered: vapor-compression refrigeration cycle (VCRC), internal heat exchanger cycle (IHEC) and ejector-expansion refrigeration cycle (EERC).

2.1. Ejector–Expansion Refrigeration Cycle

Figure 1 depicts a P-h diagram and schematic of the trans-critical N_2O cycle with an ejector system. The system includes a gas cooler, compressor, ejector, evaporator, expansion valve and vapor–liquid separator.

The saturated N_2O enters the compressor at state (1) at pressure P_s and is pressurized to P_d (the high-side pressure) at state (2), with an isentropic compressor efficiency, η_c [4]. The ideal compression process follows process 1–2 s. Then, the refrigerant cools at constant pressure P_d in the gas cooler (process 2–3). The working fluid passes through an ejector nozzle with a nozzle isentropic efficiency η_n of 0.7 [4] at the following stage, expanding to a subcritical condition at state (4) at pressure P_e. The saturated secondary vapor stream enters the ejector at a pressure of P_e in accordance with state 9. The two streams mix at constant pressure and the final state of the mixture is state 5. Note that after the mixture goes through the ejector diffuser with a diffuser isentropic efficiency η_d of 0.8 [4], it recovers to the pressure P_s at state 6. Subsequently, the mixture enters the vapor–liquid separator.

The vapor component enters the compressor at state (1), while the liquid enters expansion valve at state (7), where its pressure is reduced through an isenthalpic process. Then, refrigerant is evaporated isobarically in the evaporator via process 8–9.

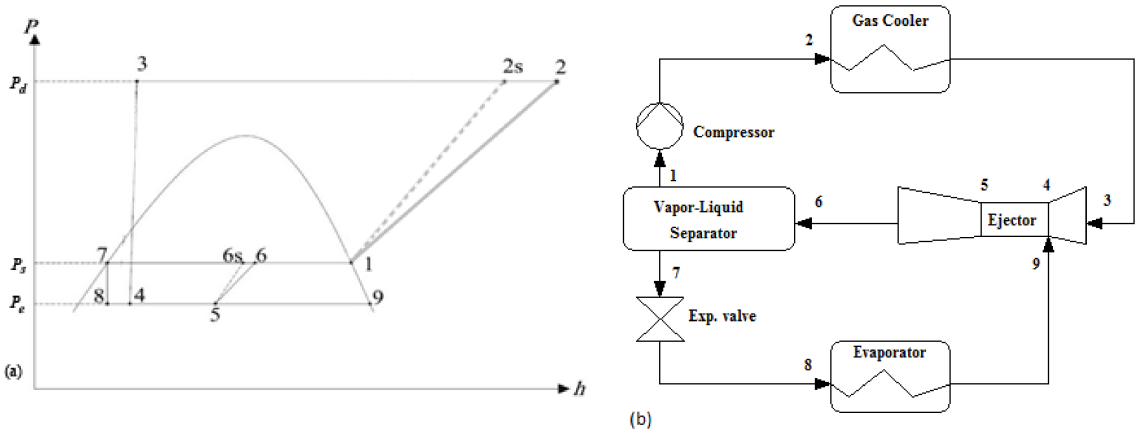

Figure 1. (**a**) *P-h* diagram; and (**b**) schematic of the trans-critical N_2O cycle with an ejector expansion system.

2.2. Vapor-Compression Refrigeration Cycle (VCRC), Internal Heat Exchanger Cycle (IHEC)

Figures 2 and 3 illustrate a P-h diagram and schematic of the vapor-compression refrigeration cycle and the internal heat exchanger cycle.

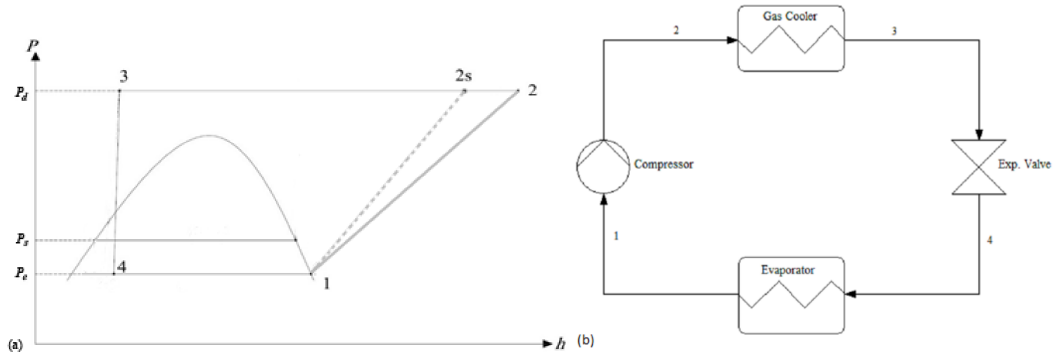

Figure 2. (**a**) P-h diagram; and (**b**) schematic of the vapor-compression refrigeration cycle.

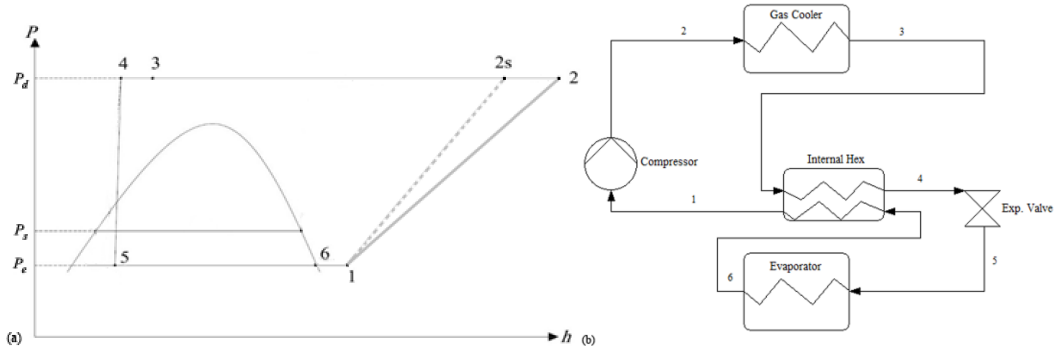

Figure 3. (**a**) P-h diagram; and (**b**) schematic of the internal heat exchanger cycle.

2.3. Assumptions

In the comparison of the three types of trans-critical N_2O cycles, several assumptions are invoked:

- All processes are at steady state and there are no flow losses within the system.
- Pressure drops in pipes and heat exchangers are negligible [4,7,8,17].
- There is no heat loss from the compressor.
- The fluid undergoes a constant enthalpy process in the expansion valve.
- The N_2O at the inlet of the compressor and the outlet of the evaporator is a saturated vapor.
- The mixing process in the mixing chamber occurs at a constant evaporation pressure.
- Changes in the potential and kinetic energies at the outlet and inlet of components are negligible.
- The dead state temperature for the analysis is 35 °C.
- The heat sink temperature is 5 °C higher than the evaporation temperature.

3. System Modelling

3.1. Energy Analysis

To model the system with the applied assumptions, the ejector entrainment ratio (U) is considered as the mass ratio of saturated vapor leaving the evaporator at state (9) to the N_2O entering the ejector nozzle. That is,

$$U = \frac{\dot{m}_9}{\dot{m}_3} \tag{1}$$

Thus, for a 1 kg/s of N_2O which flows to the separator, the suction and motive mass flow rates, respectively, are as follows [4]:

$$\dot{m}_9 = \frac{U}{U+1} \tag{2}$$

$$\dot{m}_3 = \frac{1}{U+1} \tag{3}$$

Applying energy and mass conservation laws to devices, the basic energy equations are given in Table 1. Moreover, coefficient of performance (COP) can be expressed as [4,8]:

$$COP = \frac{\dot{Q}_{eva}}{\dot{W}_c} \tag{4}$$

3.2. Exergy Analysis

The entropy generation rate through a fixed control volume and the physical exergy per unit mass, respectively, can be written, neglecting kinetic and potential energies, as follows [25]:

$$\dot{S}_{gen} = \sum \dot{m}_e S_e - \sum \dot{m}_i S_i - \sum \frac{\dot{Q}_K}{T_K} \tag{5}$$

$$\psi = (h_i - h_0) - T_0(s_i - s_0) \tag{6}$$

Thus, the exergy destruction rate can be written as follows [25]:

$$\dot{I} = T_0 \dot{S}_{gen} \tag{7}$$

The general energy as well as exergy destruction rate equations applied to each component in the three configurations of the trans-critical N_2O refrigeration cycle lead to the expressions listed in Tables 1–3 [4,8].

Table 1. Thermodynamic equations of the trans-critical N_2O cycle with an ejector expansion system.

Unit	Energy Equations	Exergy Destruction Equations
Compressor	$\eta_c = 1.003 - 0.121\left(\frac{P_d}{P_s}\right)$, $\eta_c = \frac{h_{2s}-h_1}{h_2-h_1}$ $W_c = \frac{h_2-h_1}{U+1}$	$I_c = \frac{1}{U+1}[T_0(s_2 - s_1)]$
Gas cooler	$Q_{gc} = \frac{h_2-h_3}{U+1}$	$I_{gc} = \frac{[(h_2-h_3)-T_0(s_2-s_3)]}{U+1}$
Ejector	$\eta_n = \frac{h_3-h_4}{h_3-h_{4s}}$, $\frac{v_4^2}{2} = h_3 - h_4$ $v_5 = \frac{1}{U+1}v_4$, $x_6 = \frac{1}{U+1}$, $\eta_d = \frac{h_{6s}-h_5}{h_6-h_5}$, $\frac{v_5^2}{2} = h_6 - h_5$, $h_6 = \frac{h_3}{U+1} + \frac{U}{U+1}h_9$	$I_{ejector} = \left[s_6 - \frac{s_3}{U+1} - \frac{U}{U+1}s_9\right]$
Expansion valve	$h_7 = h_8$	$I_{exp} = \frac{U}{U+1}[T_0(s_8 - s_7)]$
Evaporator	$Q_{eva} = \frac{U}{U+1}(h_9 - h_8)$	$I_{eva} = \frac{U}{U+1}T_0\left[(s_9 - s_8) - \frac{(h_9-h_8)}{T_r}\right]$

Table 2. Thermodynamic equations of the vapor-compression refrigeration cycle.

Unit	Energy Equations	Exergy Destruction Equations
Compressor	$\eta_c = 1.003 - 0.121\left(\frac{P_d}{P_e}\right)$, $\eta_c = \frac{h_{2s}-h_1}{h_2-h_1}$ $W_c = h_2 - h_1$	$I_c = T_0(s_2 - s_1)$
Gas cooler	$Q_{gc} = h_2 - h_3$	$I_{gc} = (h_2 - h_3) - T_0(s_2 - s_3)$
Expansion valve	$h_3 = h_4$	$I_{exp} = T_0(s_4 - s_3)$
Evaporator	$Q_{eva} = h_1 - h_4$	$I_{eva} = T_0\left[(s_1 - s_4) - \frac{(h_1-h_4)}{T_r}\right]$

Table 3. Thermodynamic equations of the internal heat exchanger cycle.

Unit	Energy Equations	Exergy Destruction Equations
Compressor	$\eta_c = 1.003 - 0.121\left(\frac{P_d}{P_e}\right)$, $\eta_c = \frac{h_{2s}-h_1}{h_2-h_1}$ $W_c = h_2 - h_1$	$I_c = T_0(s_2 - s_1)$
Gas cooler	$Q_{gc} = h_2 - h_3$	$I_{gc} = (h_2 - h_3) - T_0(s_2 - s_3)$
Internal Hex	$\varepsilon_{Hex} = \frac{h_1-h_6}{h_3-h_6}$	$I_{Hex} = [(h_3 - h_4) - T_0(s_3 - s_4)] -$ $[(h_1 - h_6) - T_0(s_1 - s_6)]$
Expansion valve	$h_4 = h_5$	$I_{exp} = T_0(s_5 - s_4)$
Evaporator	$Q_{eva} = h_6 - h_5$	$I_{eva} = T_0\left[(s_6 - s_5) - \frac{(h_6-h_5)}{T_r}\right]$

4. Results and Discussion

The same case has been developed based on CO_2 as the working fluid for these types of cycles, to permit comparisons with the models proposed by Deng et al. [4].

Figure 4 compares the coefficient of performance values for all CO_2 cycles developed in this paper. As shown, the results are approximately in line with those from the proposed model in reference [4].

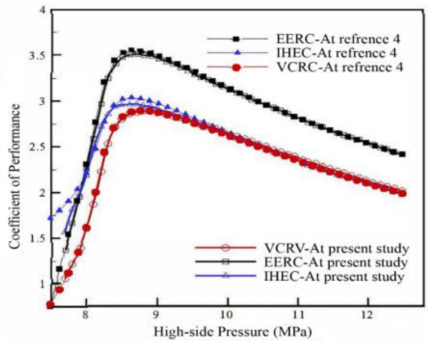

Figure 4. Validation of the proposed model based on CO_2 as the working fluid for three types of cycles.

A simulation of the three types of the cycles using the working fluid N_2O is performed. The operating conditions for these types of cycles are given in Tables 4–6.

4.1. Ejector Entrainment Ratio Analysis

An important parameter in ejector-expansion cycles is the entrainment ratio, which represents the proportion of vapor and liquid in the outlet of ejector. The importance of this ratio is so great that non-compliance with it can noticeably affect the performance of the compressor and separator and lead to unsteady system behavior [4].

Table 4. State quantities for the vapor-compression N_2O trans-critical refrigeration cycle at the following conditions: $T_{eva} = 5\ ^{\circ}C, T_{gc} = 36\ ^{\circ}C, T_{amb} = 35\ ^{\circ}C,\ P_{gc} = 8.5$ MPa.

State	T (°C)	P (MPa)	h (kJ/kg)	s (kJ/kg. K)	X	$\dot{m}$ (kg/s)
1	5	3.53	396.3	1.54	1	1
2	80.25	8.5	444.6	1.58	-	1
3	36	8.5	254	0.99	-	1
4	5	3.53	254	1.03	0.35	1

Table 5. State quantities for the internal heat exchanger N_2O trans-critical cycle at the following conditions: $T_{eva} = 5\ ^{\circ}C, T_{gc} = 36\ ^{\circ}C, T_{amb} = 35\ ^{\circ}C,\ P_{gc} = 8.5$ MPa.

State	T (°C)	P (MPa)	h (kJ/kg)	s (kJ/kg. K)	X	$\dot{m}$ (kg/s)
1	34.4	3.53	439.9	1.69	-	1
2	119.6	8.5	502.8	1.74	-	1
3	36	8.5	254	0.99	-	1
4	21.5	8.5	210.4	0.85	-	1
5	5	3.53	210.4	0.87	0.15	1
6	5	3.53	396.3	1.54	1	1

Table 6. State quantities for the ejector expansion N_2O trans-critical refrigeration cycle at the following conditions: $T_{eva} = 5\ ^{\circ}C, T_{gc} = 36\ ^{\circ}C, T_{amb} = 35\ ^{\circ}C,\ P_{gc} = 8.5$ MPa.

State	T (°C)	P (MPa)	h (kJ/kg)	s (kJ/kg. K)	X	$\dot{m}$ (kg/s)
1	8.5	3.86	394.4	1.52	1	0.6
2	75	8.5	435.1	1.55	-	0.6
3	36	8.5	254	0.99	-	0.6
4	5	3.53	246.9	1.01	0.32	0.6
5	5	3.53	308.3	1.22	0.59	1
6	8.5	3.86	310.8	1.23	0.60	1
7	8.5	3.86	185	0.781	0	0.4
8	5	3.53	185	0.783	0.04	0.4
9	5	3.53	396.3	1.54	1	0.4

Figure 5 depicts the variation of entrainment ratio and vapor quality at state (6) for trans-critical N_2O refrigerant with high-side pressure, for three evaporation temperatures. The entrainment ratio increases greatly during the first small rise in compressor discharge pressure starting at 7 MPa, and then experiences a moderate rise as the pressure increases further. This also holds true for the vapor quality at the outlet of the ejector diffuser, except that the changes are declines. In fact, the entrainment ratio and vapor quality are related and vapor quality can be calculated as a function of entrainment ratio, and vice versa. Furthermore, an increased evaporation temperature leads to a higher entrainment ratio and a lower vapor quality. The sharp variations in these results are attributed to the thermodynamic properties changes in the vicinity of N_2O critical point.

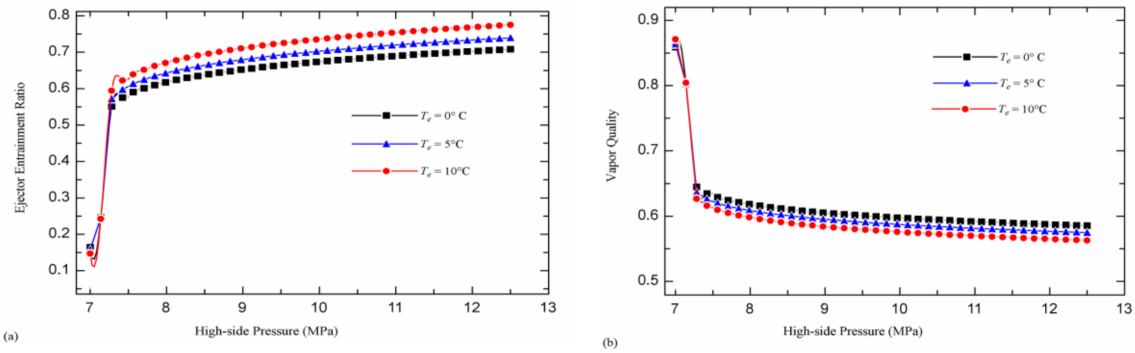

Figure 5. Variation with compressor discharge pressure of: (**a**) entrainment ratio; and (**b**) vapor quality.

Figure 6 illustrates the variation of system COP and the temperature and pressure at the ejector outlet as the ejector entrainment ratio changes, for three evaporation temperatures. It is observed in Figure 6a that, as the entrainment ratio rises (due to rising compressor discharge pressure), the system coefficient of performance rises to a peak and then sharply decreases. The optimum COP occurs approximately between entrainment ratios of 0.55 and 0.65. Although the entrainment ratio may become too low, the system remains stable with lower COPs. As the entrainment ratio rises, Figure 6b shows that the pressure and temperature of the ejector outlet decreases to a minimum and then slightly increases. Moreover, as illustrated in Figure 5b, a decrease in the vapor quality leads to a higher proportion of fluid in liquid form entering the evaporator, while less vapor passes through the compressor, which reduces the compressor work. That is, the compressor pressurizes a fluid with a higher density. Meanwhile, a lower fraction of fluid entering compressor requires less compressor work. Therefore, the coefficient of performance increases in a constant cycle refrigeration rate. As a result, all units of the system should be carefully matched with the entrainment ratio not only to achieve the most practical entrainment ratio but also to achieve the maximum coefficient of performance.

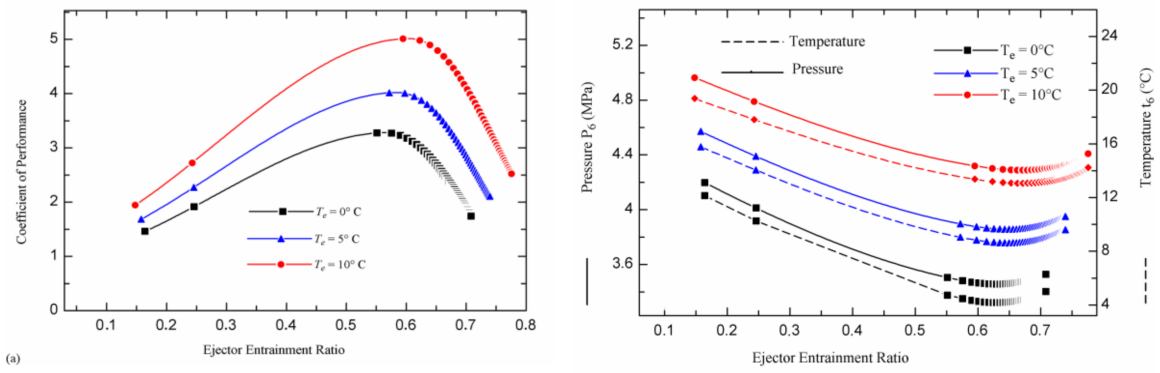

Figure 6. Variation with entrainment ratio of: (**a**) COP; and (**b**) pressure and temperature of ejector outlet.

4.2. Comparison of Three Trans-critical N_2O Refrigeration Cycles

The cycles are compared based on the model described in Section 3. Figure 7 compares the variations of coefficient of performance and exergy efficiency for three system configurations with compressor discharge pressure, for the same assumed conditions. Note that the exergy efficiency is expressed as [4,8]:

$$\eta_{ex} = \frac{\dot{W}_{rev}}{\dot{W}_c} \tag{8}$$

As shown in Figure 7, the EERC achieves the highest coefficient of performance and exergy efficiency, with values that on average are about 0.43 and 0.04 greater than the corresponding values for the IHEC, and about 0.45 and 0.04 greater than the corresponding values for the VCRC. The highest COP and exergy efficiency for all configurations above occurs for a pressure of about 7.3 MPa. Therefore, all the systems attain an optimum coefficient of performance and exergy efficiency between 7 and 7.5 MPa.

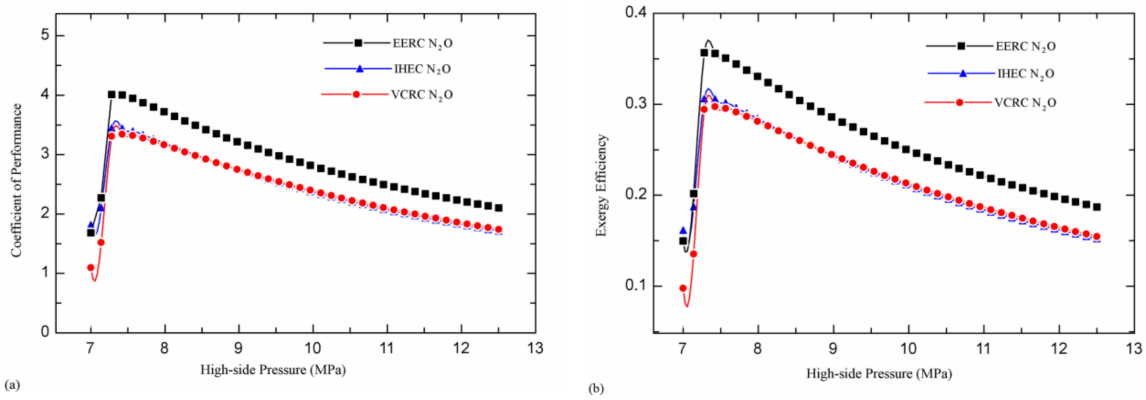

Figure 7. Variation with compressor discharge pressure of: (**a**) COP; and (**b**) exergy efficiency of the system, for three system configurations.

As shown in Figure 8, the high-side pressure corresponding to the highest COP for all cycles is about 7.3 MPa with an entrainment ratio of 0.58 for the EERC, whereas, for the CO_2 refrigerant, the high-side pressure corresponding to the highest COP is about 8.5 MPa (Figure 4). Thus, the N_2O cycle compressor consumes much less power to pressurize the working fluid. Table 7 lists the exergy destructions in all systems for a high-side pressure of 7.3 MPa and 1 kg/s of N_2O, for the three system configurations. The total exergy destruction for the N_2O ejector-expansion cycle is 63% and 53% less than for the IHEC and the VCRC, respectively. The exergy destroyed in the expansion process is 19% and 40% lower than the total exergy destruction in than IHEC and VCRC, respectively. As a result, the ejector can decrease significantly the exergy destruction associated with the throttling process in the expansion valves by reducing the pressure difference between the inlet and outlet of the expansion valve. Furthermore, Table 7 illustrates the total exergy destruction in the same cycles using CO_2 as the working fluid. The exergy destructions are lower for the EERC, IHEC and VCRC employing N_2O in comparison with those for the cycles using CO_2 which means that using N_2O as a working fluid is more practical than using CO_2 for these refrigeration systems.

Table 7. Exergy destructions in the three types of N_2O refrigeration cycles for a high-side pressure of 7.3 MPa.

Device	EERC			IHEC			VCRC		
	Loss (kJ)	**(%)**	**Loss/ex_{eva}**	**Loss (kJ)**	**(%)**	**Loss/ex_{eva}**	**Loss (kJ)**	**(%)**	**Loss/ex_{eva}**
Compressor	4.02	32.46	0.58	10.08	29.77	0.67	8.74	32.69	0.77
Gas cooler	1.98	15.96	0.29	11.30	33.38	0.75	4.25	15.92	0.35
Ejector	4.68	37.79	0.68	-	-	-	-	-	-
Exp. valve	0.19	1.55	0.03	7.09	20.94	0.48	11.25	42.05	1.03
Evaporator	1.51	12.22	0.22	3.29	9.74	0.22	2.49	9.33	0.22
Internal HX	-	-	-	2.08	6.15	0.14	-	-	-
Overall (N_2O cycle)	12.40	100	1.80	33.85	100	2.26	26.75	100	2.37
Overall (CO_2 cycle) *	13.65	100	2.20	38.05	100	2.74	30.92	100	2.94

* The total exergy destruction for the three types of CO_2 refrigeration cycle for a high-side pressure of 8.5 MPa.

4.3. Comparison of Three Cycle Types Using Trans-critical N_2O and CO_2 Working Fluids

To better compare the utilization of N_2O and CO_2 as working fluids, Figure 8 illustrates the maximum coefficient of performance and maximum exergy efficiency of the three types of the cycles using both working fluids. Each of the cycles employing N_2O exhibits a higher COP and exergy efficiency compared to the cycles employing CO_2. The maximum COP and maximum exergy efficiency for the EERC using N_2O are higher than the corresponding values for the IHEC employing the same working fluid by about 12% and 15%, while the maximum COP and exergy efficiency are 14% and 16.5% higher than corresponding values for the VCRC using N_2O.

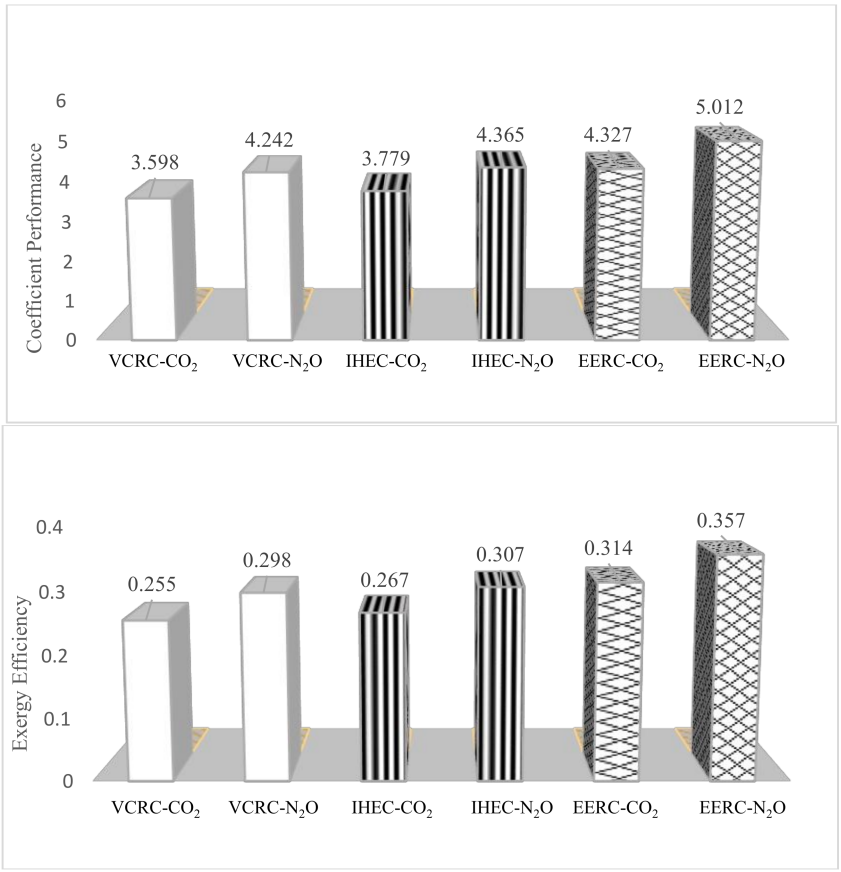

Figure 8. (**a**) COP; and (**b**) exergy efficiency values for various cycles for two working fluids.

The optimum high-side pressure of the ejector expansion refrigeration cycle and the corresponding maximum COPs and exergy efficiency are listed in Tables 8 and 9 for the cycles using N_2O and CO_2 refrigerants, respectively.

A linear regression procedure is applied to the data in Table 9 to obtain correlations for the following parameters: optimum high-side pressure, maximum COP and maximum exergy efficiency related to condenser and evaporator temperature. The resulting correlations are as follows:

$$P_{opt} = -0.676 - 0.0019T_{eva} + 0.2225T_{gc} \quad (9)$$

$$COP_{max} = 11.546 + 0.1456T_{eva} - 0.2275T_{gc} \quad (10)$$

$$\eta_{II,max} = 1.0607 - 0.00101T_{eva} - 0.0195T_{gc} \quad (11)$$

Table 8. Optimum high-side pressure of ejector-expansion refrigeration cycle (EERC) for CO_2 refrigerant and its corresponding maximum COP and η_{ex} for various design parameters.

T_{gc} (°C)	T_{eva} (°C)	$P_{OPT,High-side}$ (MPa)	COP_{max}	$\eta_{ex,max}$ (%)
36	0	8.678	2.89	31.4
	5	8.637	3.51	31.2
	10	8.658	4.33	30.3
38	0	9.128	2.61	28.3
	5	9.128	3.14	28.0
	10	9.120	3.82	26.7
40	0	9.573	2.37	25.7
	5	9.585	2.83	25.2
	10	9.584	3.40	23.8

Table 9. Optimum high-side pressure of ejector-expansion refrigeration cycle (EERC) for N_2O refrigerant and its corresponding maximum COP and η_{ex} for various design parameters.

T_{gc} (°C)	T_{eva} (°C)	$P_{OPT,High-side}$ (MPa)	COP_{max}	$\eta_{ex,max}$ (%)
36	0	7.335	3.28	35.6
	5	7.327	4.02	35.7
	10	7.314	5.01	35.1
38	0	7.786	2.91	31.6
	5	7.779	3.53	31.4
	10	7.766	4.34	30.4
40	0	8.222	2.61	28.3
	5	8.219	3.15	28.0
	10	8.206	3.82	26.7

5. Conclusions

An ejector expansion refrigeration cycle employing N_2O as the working fluid was investigated, and energy and exergy analyses were carried out. The effects of key factors on system performance were determined and this system was compared with others employing the same refrigerant as well as systems using CO_2 as the working fluid. Furthermore, the results from this study were validated using results for similar systems proposed in other studies using CO_2 as the working fluid. Three types of cycles are considered: vapor-compression refrigeration cycle (VCRC), internal heat exchanger cycle (IHEC) and ejector-expansion refrigeration cycle (EERC). The results for the cycles using N_2O showed that the ejector entrainment ratio, one of the important parameters in ejector-expansion cycles representing the proportion of vapor and liquid in the outlet of ejector, varies significantly with high-side pressure of the cycle the quality in the outlet of the ejector. Increasing entrainment ratio by raising compressor discharge pressure causes the coefficient of performance to increase to a peak and then sharply decrease. Moreover, coefficient of performance for the cycle exhibits an optimum value for the different evaporation cycles and a higher evaporation temperature results in a higher system COP. This variation is the opposite of that observed for the cycle using N_2O. Then, the temperature and pressure at the outlet of the ejector smoothly decline to a minimum as the entrainment ratio increases. The comparison between three types of N_2O refrigeration cycles shows that the maximum coefficient of performance for the cycles occurs at roughly the same high side pressure, and that the maximum value is exhibited by the EERC cycle. The same occurs for exergy efficiency of the cycles. The highest COP in this study corresponds to a high side pressure of 7.3 MPa for three types of N_2O refrigeration cycles, but about 8.5 MPa for three types of CO_2 refrigeration cycles. Consequently, the compressor in the N_2O systems requires less work to pressurize the working fluid in the system. The exergy analysis also identifies the exergy destroyed in the system in three types of cycles. The total exergy destruction in the N_2O ejector-expansion cycle was seen to be 63% and 53% less than the values for the IHEC and VCRC, respectively. A comparison of the total exergy destruction is also made between the

cycles using CO_2 and N_2O working fluids. The results show that there is less exergy destruction in the EERC, IHEC and VCRC employing N_2O than in those using CO_2, which means that using N_2O is better than CO_2 for these refrigeration systems. To enhance the comparison, the maximum COP and exergy efficiency of the three types of cycles using both working fluids were examined. It was seen that these parameters are higher for the EERC than the IHEC and VCRC, and that each type of cycle employing N_2O has a higher COP and exergy efficiency than the corresponding cycle using CO_2. Further, the maximum COP and exergy efficiency for the EERC using N_2O are higher than those values for the IHEC employing the same working fluid by about 12% and 15%, respectively. Meanwhile the maximum COP and exergy efficiency are 14% and 16.5% higher than VCRC using N_2O, respectively. Thus, this leads to an optimal cooling system with lower power consumption in compressor. Finally, linear regression is applied to determine the optimum high-side pressure, the maximum COP and the maximum exergy efficiency, as functions of the gas cooler and evaporator temperatures.

Acknowledgments: We have not received any fund for this work.

Author Contributions: The work is conducted and wrote by D.A. Dokandari under supervision of S.M.S. Mahmoudi, M. Bidi, R.H. Khoshkhoo and Marc A. Rosen.

Conflicts of Interest: The authors declare no conflict of interest.

Nomenclature

Ψ	Specific stream exergy (kJ/kg)
η	Efficiency
ε	Heat exchanger effectiveness (%)
COP	Coefficient of performance
ex	exergy (kJ)
h	Specific enthalpy (kJ/kg)
$\dot{I}$	Exergy destruction rate (kW)
$\dot{m}$	Mass flow rate (kg/s)
P	Pressure (MPa)
$\dot{Q}$	Heat transfer rate (kW)
s	Specific entropy (kJ/kg K)
$\dot{S}$	Entropy generation rate (kW/K)
T	Temperature (°C)
U	Entrainment ratio of ejector
v	Velocity (m/s)
$\dot{W}$	Work rate (kW)
x	Quality (kg/kg)
Subscripts	
amb	Ambient
c	Compressor
d	Discharge pressure of ejector; Diffuser
eva /e	Evaporator
exp	Expansion valve
gc	Gas cooler
gen	Generation
Hex	Heat Exchanger
n	Ejector nozzle
r	Heat sink temperature
s	Vapor–liquid separator
0	Dead state of system

References

1. Calm, J.M. The next generation of refrigerants–historical review, considerations and outlook. *Int. J. Refrig.* **2008**, *31*, 1123–1133. [CrossRef]
2. Bhattacharyya, S.; Garai, A.; Sarkar, J. Thermodynamic analysis and optimization of a novel N_2O-CO_2 cascade system for refrigeration and heating. *Int. J. Refrig.* **2009**, *32*, 1077–1084. [CrossRef]
3. Kruse, H.; Rüssmann, H. The natural fluid nitrous oxide—an option as substitute for low temperature synthetic refrigerants. *Int. J. Refrig.* **2006**, *29*, 799–806. [CrossRef]
4. Deng, J.; Jiang, P.; Lu, T.; Lu, W. Particular characteristics of transcritical CO_2 refrigeration cycle with an ejector. *Appl. Therm. Eng.* **2007**, *27*, 381–388. [CrossRef]
5. Sadeghi, M.; Yari, M.; Mahmoudi, S.M.S.; Jafari, M. Thermodynamic analysis and optimization of a novel combined power and ejector refrigeration cycle – Desalination system. *Appl. Energy.* **2017**, *208*, 239–251. [CrossRef]
6. Ünal, S.; Erdinç, M.T.; Kutlu, C. Optimal thermodynamic parameters of two-phase ejector refrigeration system for buses. *Appl. Therm. Eng.* **2017**, *124*, 1354–1367. [CrossRef]
7. Sarkar, J.; Bhattacharyya, S. Thermodynamic analyses and optimization of a transcritical N_2O refrigeration cycle. *Int. J. Refrig.* **2010**, *33*, 33–40. [CrossRef]
8. Aghazadeh Dokandari, D.; Setayesh Hagh, A.; Mahmoudi, S.M.S. Thermodynamic investigation and optimization of novel ejector-expansion CO_2/NH_3 cascade refrigeration cycles (novel CO_2/NH_3 cycle). *Int. J. Refrig.* **2014**, *46*, 26–36. [CrossRef]
9. Croquer, S.; Poncet, S.; Galanis, N. Comparison of ejector predicted performance by thermodynamic and CFD models. *Int. J. Refrig.* **2016**, *68*, 28–36. [CrossRef]
10. Sarkar, J.; Bhattacharyya, S. Optimization of a transcritical N_2O refrigeration/heat pump cycle (NIK-06-T1-14). In Proceedings of the 8th IIR G Lorentzen Conference on Natural Working fluids, Copenhagen, Denmark, 7–10 September 2008.
11. Sarkar, J.; Bhattacharyya, S.; Ramgopal, M. Optimization of a transcritical CO_2 heat pump cycle for simultaneous cooling and heating applications. *Int. J. Refrig.* **2004**, *27*, 830–838. [CrossRef]
12. Sarkar, J.; Bhattacharyya, S.; Ramgopal, M. Natural refrigerant-based subcritical and transcritical cycles for high temperature heating. *Int. J. Refrig.* **2007**, *30*, 3–10. [CrossRef]
13. Seckin, C. Thermodynamic analysis of a combined power/refrigeration cycle: Combination of Kalina cycle and ejector refrigeration cycle. *Energy Convers. Manag.* **2018**, *157*, 631–643. [CrossRef]
14. Lee, T.S.; Liu, C.H.; Chen, T.W. Thermodynamic analysis of optimal condensing temperature of cascade-condenser in CO_2/NH_3 cascade refrigeration systems. *Int. J. Refrig.* **2006**, *29*, 1100–1108. [CrossRef]
15. Carrillo, J.A.E.; Sanchez de la flor, F.J.; Salmeron Lissen, J.M. Thermodynamic comparison of ejector cooling cycles. Ejector characterisation by means of entrainment ratio and compression efficiencys. *Int. J. Refrig.* **2017**, *74*, 371–384. [CrossRef]
16. Rashidi, M.M.; Aghagoli, A.; Raoofi, R. Thermodynamic analysis of the ejector refrigeration cycle using the artificial neural network. *Int. J. Energy* **2017**, *129*, 201–215. [CrossRef]
17. Yari, M.; Mahmoudi, S.M.S. Thermodynamic analysis and optimization of novel ejector-expansion TRCC (transcritical CO_2) cascade refrigeration cycles (Novel transcritical CO_2 cycle). *Int. J. Energy.* **2011**, *36*, 6839–6850. [CrossRef]
18. Yari, M. Performance analysis and optimization of a new two-stage ejector-expansion transcritical CO_2 refrigeration cycle. *Int. J. Therm. Sci.* **2009**, *48*, 1997–2005. [CrossRef]
19. Ghaebi, H.; Parikhani, T.; Rostamzadeh, H.; Farhang, B. Thermodynamic and thermoeconomic analysis and optimization of a novel combined cooling and power (CCP) cycle by integrating of ejector refrigeration and Kalina cycles. *Int. J. Energy.* **2017**, *139*, 262–276. [CrossRef]
20. Jeon, Y.; Dongwoo, J.; Sunjaekim, K.; Kim, Y. Effects of ejector geometries on performance of ejector-expansion R410A air conditioner considering cooling seasonal performance factor. *Appl. Energy* **2017**, *205*, 761–768. [CrossRef]
21. Zhu, Y.; Jiang, P. Theoretical model of transcritical CO_2 ejector with non-equilibrium phase change correlation. *Int. J. Refrig.* **2018**, *86*, 218–227. [CrossRef]
22. Fang, Y.; Croquer, S.; Poncet, S.; Bartosiewicz, Y. Drop-in replacement in a R134 ejector refrigeration cycle by HFO refrigerantsRemplacement. *Int. J. Refrig.* **2017**, *17*, 87–98. [CrossRef]

23. Ma, Z.; Bao, H.; Roskilly, A.H. Thermodynamic modelling and parameter determination of ejector for ejection refrigeration systems. *Int. J. Refrig.* **2017**, *75*, 117–128. [CrossRef]
24. Choudhary, K.; Dasgupta, M.S.; Sunder, S. Energetic and exergetic investigation of a N_2O ejector expansion transcritical refrigeration cycle. *Int. J. Energy Procedia* **2017**, *109*, 122–129. [CrossRef]
25. Dincer, I.; Rosen, M.A. *Exergy: Energy, Environment and Sustainable Development*, 2nd ed.; Elsevier: New York, NY, USA, 2013.